# PRACTICAL APPLICATION OF A MODEL FOR FATIGUE DAMAGE WITH IRREGULAR CYCLIC LOADING

H. Führing

Fraunhofer-Institut für Betriebsfestigkeit (LBF)
Darmstadt, F.R. Germany

## ABSTRACT

The new developed load-sequence model for fatigue crack growth takes nonlinear effects such as retardation, acceleration and multiple load interaction into account. Working on a cycle-by-cycle basis the model uses a modified stress intensity range in the normal crack propagation law. The modification is made by multiplying $\Delta K$ by an acceleration and a retardation factor which both are governed by the development of elasto-plastic boundaries obtained under small scale / strip yielding assumptions.
After being successfully applied to simple irregular load sequences, e.g. single peak overloading (Führing, 1980), the model which uses only basic material data is now being checked against a realistic load spectrum. Detailed information on the comparison of test results with crack growth predictions after the conventional linear theory as well as the load-sequence model is given which exemplifies the improvement in prediction accuracy of the new model.

## KEYWORDS

Fatigue crack growth; acceleration/retardation effect; prediction model; spectrum loading; small scale yielding; plastic zones.

## INTRODUCTION

The conventional cycle-by-cycle crack growth analysis is based on the assumption that the increasing part of a full cycle causes the same crack growth increment as a constant amplitude (CA) cycle of equal magnitude. From the fact that only quantities of linear elastic fracture mechanics are used the terms "linear theory" or "$\Delta K$ method" are in use for the conventional prediction technique when applied to spectrum loading. Figure 1 shows a cut-out of a typical load-time record and, schematically, the related experimental crack growth curve. At two distinctive events the crack growth rate as expected after linear theory is compared with the experimentally observed crack growth rate. One event is characterised by a retardation, the other one by an acceleration of the crack growth. With spectrum loading numerous accelerations and retardations interact and superimpose each other. Both these non-

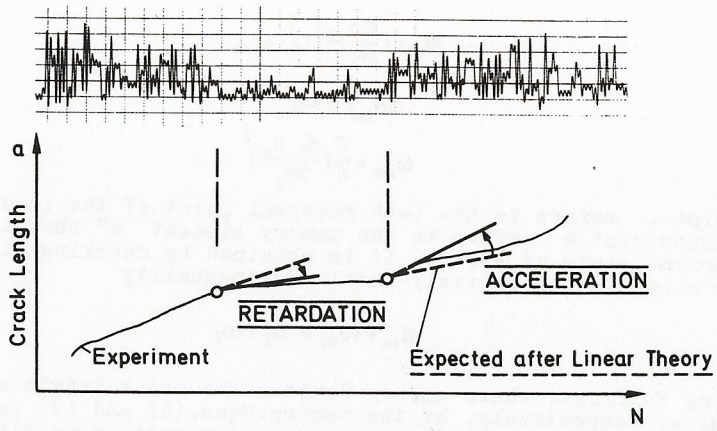


Fig. 1 Nonlinear crack growth effects

linear effects have been known for many years, however, difficulties arise if retardation or acceleration are to be quantified under generalised conditions. By linear theory, the crack growth life of most practical cases is drastically underestimated, i.e. by a factor of 4 and above. To take this into account several retardation models had been established in the past, e.g. the Wheeler (1972) and the Willenborg (1971) model. However, those models have the disadvantage that they must be adjusted for each particular problem area. In fact, the constants they use are material and load-history dependent because the models neither account for acceleration effects nor for multiple load interaction. Both features are incorporated in the new model.

Table 1 gives a summary of three crack growth models on which the author worked. The table is arranged from the left to the right hand side in a decreasing order of physical relevance. The local strain model (Seeger, 1973) as well as the effective stress range model (Elber, 1971) which both account for the important fatigue crack closure mechanism were successfully used for basic studies (Führing, 1977). However, cyclewise continuum mechanics analyses of the parameters $\Delta v_a$ and $U$ are too expensive when considering spectrum loading. On the other hand, the interrelations between the characteristic parameters and the loading, geometry as well as the uniaxial material properties are so complicated that it is unlikely to find qualified approximation functions for the whole variety of practical problems. Therefore, the load-sequence model was established being a simple but effective general scheme which builds on closed parameter solutions under small scale / strip yielding assumptions.

As the key issue of the new model approach a modified stress intensity range $\Delta K_{LS}$ is introduced which shall describe the influence of all previous load cycles on the current damage state

$$\Delta K_{LS} = Q_{LS} \cdot \Delta K = Q_a \cdot Q_r \cdot \Delta K \qquad (1)$$

The modified stress intensity range replaces the conventional $\Delta K$ in



TABLE 1 Summary of Crack Growth Models

| Crack Growth Model | Local Strain | Effective Stress Range | Load Sequence Factor |
|---|---|---|---|
| Constant Amplitude (R=const.) | $\frac{da}{dN} = \tilde{C} \cdot \Delta v_{a,CA}^{\tilde{n}}$ $\Delta v_a \sim \Delta K_{eff}^2$ | $\frac{da}{dN} = \tilde{C} \cdot (U_{CA} \cdot \Delta K)^n$ $\frac{}{\Delta K_{eff}}$ $\tilde{C} \cdot U_{CA}^n = C$ | $\frac{da}{dN} = C \cdot (Q_{CA} \cdot \Delta K)^n$ (Paris) [or Forman] |
| Governing Variable | $\Delta v_a$: Displacement Variation of the Crack Tip Material Element | U: Effective Stress Range Ratio $U = \Delta K_{eff}/\Delta K = f(R)$ | Q: Load Sequence Factor $C = C(R)$ (Paris) |
| | | $\Delta K$: Stress Intensity Range (LEFM) | |
| ...Obtained through | – (Experimental Measurements) – FE-Calculations – Dugdale Calculations | | $Q_{CA}=1$ C(R) from Experiments |
| Spectrum Loading | $\Delta a = \tilde{C} \cdot \Delta v_{a,LS}^n$ | $\Delta a = \tilde{C} \cdot (U_{LS} \cdot \Delta K)^n$ $Q_{LS} = U_{LS}/U_{CA}$ | $\Delta a = C \cdot (Q_{LS} \cdot \Delta K)^n$ (Paris) [or Forman] |
| Variable Obtained through | (as above) Very Expensive Mostly not Performable | | Closed Solution Based on Structural and Material Data Only |

the crack growth law. It is assumed a product of two factors: an acceleration factor $Q_a$ and a retardation factor $Q_r$ which both depend only on the applied sequence of loading. At each load cycle the following two questions concerning the crack growth increment have to be answered. First, which contribution results from treating the cycle as load history independent ? - i.e. considering a CA history of equal amplitude and stress ratio. Second, how much this contribution must be enlarged or diminished due to the particular load history ?

Apparently - and quite intentionally - the present approach is built around the CA crack growth law (where $Q_a=Q_r=1$), i.e. all micro-mechanical and environmental properties of the material in consideration are assumed to be condensed in the CA data. As a consequence, the more representative the input material constants C, n for the actual application are, the better is the estimation accuracy for spectrum loading. In Table 1 certain interrelations between the Elber model and the load-sequence model are indicated which will be illuminated in the following sections where the formulae for the acceleration and retardation factor will be derived.

## RETARDATION FACTOR

Figure 2 schematically shows the result of an elasto-plastic strip-yielding analysis of a centre cracked specimen subjected to single peak overloading (Führing, 1977). Depicted are the parameters $\Delta v_a$ and $U$ (as defined in Table 1) with crack extension after overload application as well as the development of plastic zone sizes $\omega$ at maximum load. Non-regarding crack closure the local strain described by $\Delta v_a$ was always greater than that expected from pure CA loading (representing linear theory). Inserted into the local crack growth law the simple analysis without crack closure yields that crack growth will not be retarded but merely accelerated after the overload which

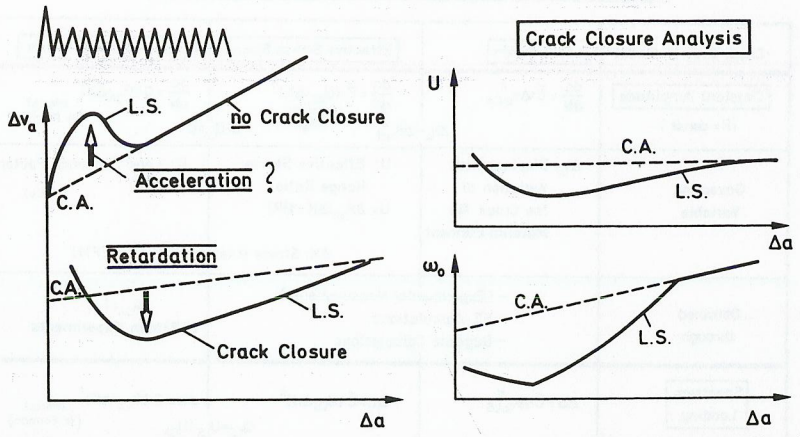


Fig. 2 Analytical parameter development after an overload

stands in apparent contradiction to common experience. In fact, $\Delta va$ values that correspond to the observed retardation effect are only obtained if crack closure is taken into account as shown by the lower left hand curve which then comes to lie below the respective CA curve.

The similarity of the U-ratio and the $\omega$-size development, see the right hand curves in Fig. 2, indicated the way how to establish the model approach. The idea behind was that the retardation effect of any type of a high-low sequence can be expressed by a ratio of two plastic zone sizes instead of the effective stress range ratio: one of them being the monotonic plastic zone size, the other being the plastic zone size as affected by the sequence of loading. The proposed formula reads

$$Q_r = \sqrt{\omega_{o,LS}/\omega_{o,CA}}/(1-R) \qquad (2)$$

For cycles with a minimum to maximum load ratio $R=S_u/S_o<0$ the (1-R)-term in expression (2) must be cancelled. Furtheron, only $Q_r$-values less or equal to one are considered. The Dugdale (1960) formula of the plasic zone size at the upper (lower) reversal points of CA loading reads

$$\omega_{o,CA} = \frac{\pi}{8}\left(\frac{K_o}{\bar{\sigma}_y}\right)^2 \qquad \omega_{u,CA} = \frac{\pi}{8}\left(\frac{\Delta K}{2\bar{\sigma}_y}\right)^2 \qquad (3)$$

where $K_o$ is the stress intensity factor at maximum load and $\sigma_y$ is the yield stress of the material

$$\bar{\sigma}_y = \sigma_y \quad \text{for plane stress,} \quad \bar{\sigma}_y = 2.5\,\sigma_y \quad \text{for plane strain} \qquad (4)$$

The plastic zone size being affected by the load sequence is (see: (Führing and Seeger, 1979, Führing, 1980) :



$$\omega_{LS} = \left(\frac{\Delta a_{i,m}}{\omega_{i,m}} - 1\right)^2 \cdot \omega_{i,m} \qquad (5)$$

where

$$\Delta a_{i,m} = a_i - a_m \qquad (6)$$

$$\omega_{i,m} = \frac{\pi}{8}\left(\frac{K_i - K_m}{2\bar{\sigma}_y}\right)^2 \qquad (7)$$

Subscript i refers to the i-th reversal point of the load-time function. Subscript m refers to the memory element $m^*$ that is valid for the current state of stress. It is obtained by checking all active memory elements successively until the inequality

$$a_m + \omega_m > a_i + \omega_i \qquad (8)$$

is being fulfilled where $a_m, \omega_m$ denotes the crack length and plastic zone size, respectively, of the memory. Eqns. (5) and (7) can be used for upper load reversals ($\omega_{o,LS}$: tensile plastic zone size, odd numbered) and lower load reversals, as well ($\omega_{u,LS}$: compressive plastic zone size, even numbered). The damage of cycles lying fully in compression is neglected. For cycles with lower reversals in compression, $S_u<0$, the plastic zone size is to calculate using a corrected minimum load

$$\tilde{S}_u = \left(1-\sqrt{0.2(1-R)^2+0.8}\right) S_o \qquad (9)$$

## ACCELERATION FACTOR

Figure 3 shows a low-high block sequence being the most typical (but not the only) event causing acceleration. Again, continuum mechanics was able to furnish the rationale for this effect only when taking

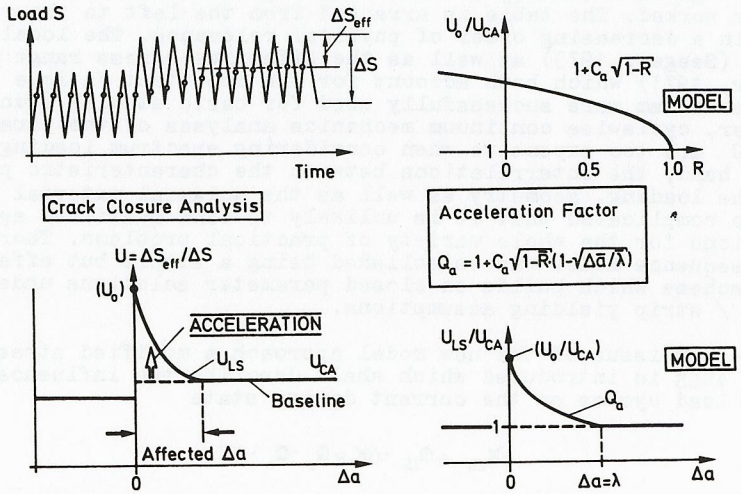


Fig. 3 Crack growth acceleration, analysis and model approach

fatigue crack closure into account. The analytical development of the crack opening load after the loading step is schematically indicated by the circles in the load-time function. The opening load approaches the stable level of the second loading block only gradually instead of jumping at the very change of loading. In terms of the effective stress range ratio U drawn in the diagram below we have a transitional curve $U_{LS}$. Its parameters are the initial value $U_O$ and the crack length increase $\Delta a$ over which the growth rate is affected. Since the acceleration effect has not yet been explored so thoroughly as the retardation effect very few information on U as a function of crack extension is available. That was the reason why an empirical constant, namely $C_a$, had to be introduced into the model for scaling the function of the initial value $U_O$. Fortunately, $C_a$ turns out to be a material constant. The final expression for the acceleration factor reads

$$Q_a = 1 + C_a \sqrt{1-\bar{R}} \cdot (1 - \sqrt{\Delta \bar{a}/\bar{\lambda}}) \qquad (10)$$

Only $Q_a$-values greater or equal to one are considered. As key assumption, the affected crack length, i.e. the acceleration influence zone was taken to be equal to the length of the contact zone $\lambda$ . The contact zone is that part of the crack surface where crack closure at minimum load occurs (Führing, 1977). The bars in Eqn. (10) are used in connection with spectrum loading. Then, a stress ratio of an "equivalent" CA loading $\bar{R}=\bar{S}_u/\bar{S}_O$ is defined with $\bar{S}_O$ ($\bar{S}_u$) being the average maximum (minimum) load within the acceleration zone. The acceleration starts at each load cycle the maximum load of which forms a plastic zone being more than 10% larger than the average plastic zone

$$\omega_{o,CA} > 1.10 \cdot \bar{\omega}_{o,CA} \qquad (11)$$

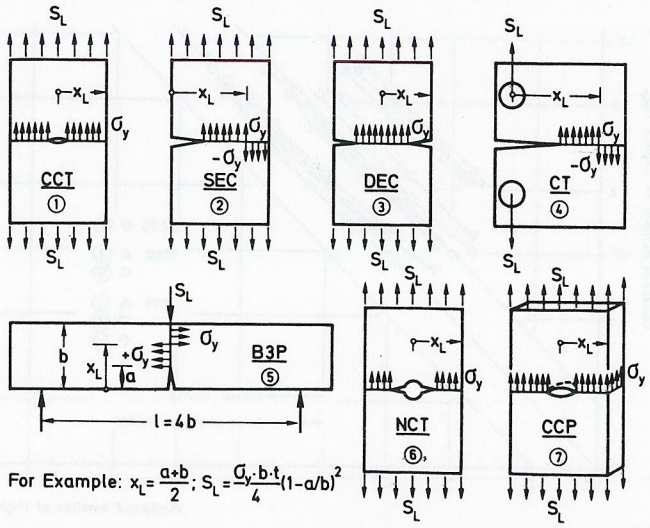


Fig. 4 Geometrical cases and states at plastic limit load



The extent of the contact zone of the equivalent CA loading can be approximated by

$$\bar{\lambda} = \left(125\,(1-a/x_L)^2 + 1.5(1-\bar{R})(S_L/\bar{S}_o)^2\right)\bar{\omega}_{u,CA}/(1-\bar{R})^2 \qquad (12)$$

with $S_L$ being the plastic limit load with respect to the current crack length and $x_L$ being the coordinate of the elasto-plastic boundary at limit load. If the $\lambda$-value calculated according to Eqn.(12) exceeds the crack length, then $\lambda$=a is used. Figure 4 illustrates the stress states at limit load for all geometrical cases that have been implemented in the computer programme up to now. In the figure the expressions for $x_L$ and $S_L$ of the three point bending (B3P) specimen are given as an example. The others can be readily derived by fulfilling the equilibrium conditions.

## PRACTICAL APPLICATION OF THE MODEL

Table 2 shows the material data of the numerical examples as taken from Sippel and Weisgerber (1975) except of the just mentioned $C_a$-value and the exponent $\bar{n}$. $\bar{n}$=1 means that the normal Forman (1966) law was applied where the crack growth increment per cycle reads

$$\Delta a = \frac{C \cdot \Delta K_{LS}^{n}}{(1-R)\cdot K_c - \Delta K_{LS}} \qquad (13)$$

For a better description of the mean load dependence the author introduced an exponent $\bar{n} \neq 1$ for the (1-R) term in Eqn.(13). This modified Forman expression was used with the alluminium alloys 7050 and AZ75. For 7050 a variety of CAtest data exist enabling a proper adjustment of $\bar{n}$,C and n while very little information on the R-ratio influence of AZ75 exists. Therefore, $\bar{n}$ was assumed equal to that of 7050. As to the recommended $C_a$-values in the table (held constant for all investigations of the same material) it can be stated that AZ75 and 7050 show no acceleration behaviour whereas aluminium 7075 exhibits a pronounced acceleration behaviour; the $C_a$-value is 0.4 being the same as for aluminium 2024.

TABLE 2 Mechanical and Fracture Mechanics Material Data (N,mm)

| Code | Material | Semifinished Product | | Mechanical Properties | | Specimen Thickness | Fracture Mechanics Properties | | | | |
|---|---|---|---|---|---|---|---|---|---|---|---|
| | | Type | Thickness | $\sigma_u$ | $\sigma_y$ | | $K_c$ | C | n | $\bar{n}$ | $C_a$ |
| A | AZ75 | Forged Plate | 60 | 476 | 401 | 6 | 2423 | $3.8\cdot10^{-5}$ | 1.67 | 0.8-0.4R | 0 |
| B1 | 7050-T73651 | Plate | 100 | 505 | 440 | 6 | 2227 | $2.00\cdot10^{-7}$ | 2.41 | 1 | 0 |
| B2 | " | " | " | " | " | | | $6.63\cdot10^{-8}$ | 2.63 | 0.8-0.4R | 0 |
| C1 | " | Plate | 150 | 523 | 457 | 6 | 1876 | $6.35\cdot10^{-8}$ | 2.57 | 1 | 0 |
| C2 | " | " | " | " | " | | | $3.65\cdot10^{-7}$ | 2.30 | 0.8-0.4R | 0 |
| D1 | 7075-T7351 | Plate | 90 | 462 | 382 | 2.5 | 1920 | $4.21\cdot10^{-7}$ | 2.25 | 1 | 0.4 |
| D2 | " | " | " | " | " | 6 | 1780 | $3.11\cdot10^{-9}$ | 3.00 | 1 | 0.4 |
| D3 | " | " | " | " | " | 9 | 1600 | $5.75\cdot10^{-9}$ | 2.91 | 1 | 0.4 |
| E1 | T16A14Vann | Forged Plate | 85 | 1001 | 959 | 2.5 | 4480 | $2.04\cdot10^{-7}$ | 2.36 | 1 | 0.1 |
| E2 | " | " | " | " | " | 5 | 3490 | $2.29\cdot10^{-8}$ | 2.69 | 1 | 0.1 |
| E3 | " | " | " | " | " | 8 | 3688 | $2.27\cdot10^{-10}$ | 3.35 | 1 | 0.1 |
| F | T16A14Vann | Rolled Plate | 83 | 908 | 847 | 5 | 4437 | $3.69\cdot10^{-7}$ | 2.32 | 1 | 0.1 |

TABLE 3 Fighter Spectrum Crack Growth Prediction (N,mm)

| Case | Material Code | Specimen Thickness | Plane Strain (1) Plane Stress (0) | Half Width b | Maximum Spectrum Load | Flights to Failure $N_f$ Experim. | Linear Theory | LOSEQ | Life Factor Linear Theory | LOSEQ |
|---|---|---|---|---|---|---|---|---|---|---|
| 1 | A | 6 | 1 | 80 | 196 | 5300 | 1020 | 3010 | 5.2 | 1.76 |
| 2 | B1 | 6 | 1 | 80 | 196 | 7850 | 1780 | 8780 | 4.4 | 0.89 |
| 3 | B2 | " | " | " | " | " | 1370 | 7780 | 5.7 | 1.01 |
| 4 | C1 | 6 | 1 | 80 | 196 | 6770 | 1580 | 8780 | 4.3 | 0.77 |
| 5 | C2 | " | " | " | " | " | 1410 | 6895 | 4.8 | 0.98 |
| 6 | D1 | 2.5 | 0 | 80 | 273 | 1260 | 580 | 1400 | 2.2 | 0.90 |
| 7 | " | " | " | " | 196 | 6950 | 1660 | 3895 | 4.2 | 1.78 |
| 8 | D3 | 9 | 1 | 80 | 196 | 5100 | 1780 | 4780 | 2.9 | 1.07 |
| 9 | D2 | 6 | 1 | 80 | 273 | 1100 | 695 | 1895 | 1.6 | 0.58 |
| 10 | " | " | " | " | 196 + | 5360 | 2210 | 6095 | 2.4 | 0.88 |
| 11 | " | " | " | " | 196 ++ | 4800 | 2295 | 6380 | 2.1 | 0.75 |
| 12 | " | " | " | " | (196)++ | 3680 | 2380 | 4580 | 1.6 | 0.80 |
| 13 | " | " | " | " | (196)+++ | 2820 | 2495 | 3000 | 1.1 | 0.94 |
| 14 | E1 | 2.5 | 0 | 80 | 549 | 1650 | 325 | 1260 | 5.1 | 1.31 |
| 15 | " | " | " | " | 373 | 6300 | 1095 | 4180 | 5.8 | 1.51 |
| 16 | E3 | 8 | 1 | 60 | 373 | 3850 | 980 | 4895 | 3.9 | 0.79 |
| 17 | E2 | 5 | 1 | 80 | 549 | 1160 | 194 | 650 | 6.0 | 1.78 |
| 18 | " | " | " | " | 373 | 3220 | 695 | 2980 | 4.6 | 1.08 |
| 19 | " | " | " | " | (373)+++ | 2320 | 780 | 1495 | 3.0 | 1.55 |
| 20 | " | " | " | " | (373)++++ | 1600 | 885 | 1170 | 1.8 | 1.37 |
| 21 | F | 5 | 1 | 80 | 373 | 5110 | 780 | 2780 | 6.6 | 1.84 |

+ Truncation of Loads < 0 ++ Truncation at 85% +++ Truncation at 72.5% ++++ Truncation at 58.5%

All the cases listed in Table 3 were experimentally tested on centre cracked tension specimen by Sippel and Weisgerber (1975). The loading was a fighter spectrum with 200 flights consisting of 14226 cycles in a period. The comparison of observed lives to predicted lives is made on the basis of flights to failure. Crack growth life is defined by propagating a crack from a half length of 2.5 mm to critical length which depends on the maximum spectrum load applied and the fracture toughness $K_c$. Predictions are made by using the computer programme LOSEQ based on the load-sequence model and by the linear theory with $\Delta K$ instead of $\overline{\Delta K}_{LS}$ in Eqn.(13), as well. The assumption concerning the stress state was: plane strain for all cases except of the 2.5 mm thin sheets.

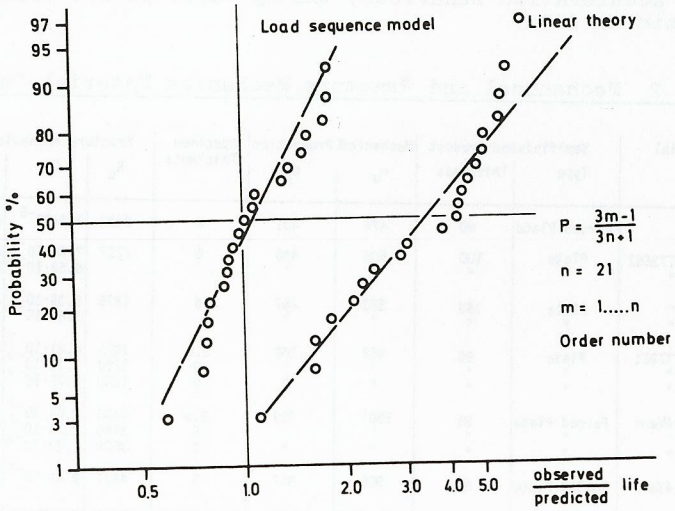


Fig. 5 Probability plot of model predictions



The computational cases 2 and 4 carried out with the Forman constants as published by Sippel and Weisgerber are to compare with cases 3 and 5, respectively. The experimentally observed lives (i.e. 7850 and 6770 flights) are predicted with more accuracy when using the modified Forman law (7780 and 6895 flights, respectively, instead of 8780 flights in both cases 2 and 4). Additionally, the comparative analysis shows that the factor of observed to predicted life according to linear theory obviously is sensitive as to the CA law applied. Figure 5 illustrates the prediction accuracy of LOSEQ in comparison with the linear theory. The symbols represent the life factors of all 21 cases investigated. The advantage of the new model can be readily seen: not only the probability curve is centered at a life factor of ~1, but the slope of the probability distribution is as steep as with many simple CA crack growth predictions ( $T=P_{10\%}/P_{90\%}=1:2.5$). On the other hand, the large scatter in life factors from linear theory (T=1:4.8) is very typical with spectrum loading cases. Figure 6 shows a plot of observed versus predicted flights representing the whole crack growth period from about 0.15 $\bar{N}_f$ to final failure. All symbols of a single computational case are connected by a line. Observing that all lines in Fig.6, those predicted by LOSEQ and those after linear theory, are approximately parallel to the diagonale it can be stated that the life factors as given in Table 3 are representative for the whole crack growth period and not only for final failure. This fact is of great importance when using the LOSEQ prediction for the estimation of inspection intervals of real structures.

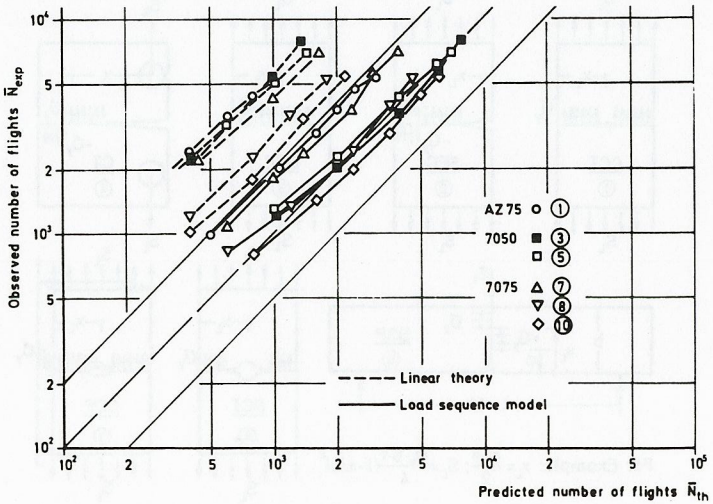


Fig. 6 Prediction accuracy with crack growth (aluminium alloys)

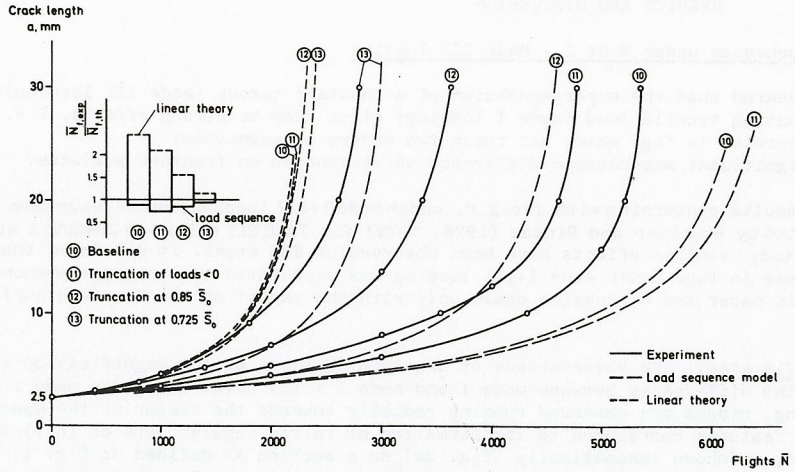


Fig. 7 Effect of load spectrum modifications (7075-T7351)

In Fig. 7 the crack length versus number of fligths curves for the modified spectrum loading are drawn (the modifications are denoted in Table 3). It is a good example for the load sequence influence on fatigue damage. Linear theory gives the same answers for all four variations while the real crack growth behaviour is affected is typically affected by truncations. The observed crack growth is modelled fairly well by the new model which yields approximately the same accuracy for all modifications.

REFERENCES

Dugdale, D. S. (1960). J. Mech. Phys. of Solids, 8, 100-104

Elber, W. (1971). Damage Tolerance of Aircraft Structures. ASTM - STP 486, 230-242

Forman, R.G., V. E. Kearney, and R. M. Engle (1966). Trans. ASME, J. Basic Eng., 459-

Führing, H. (1977). Elastic-plastic crack closure analysis of Dugdale crack plates based on fatigue fracture mechanics (in german). Report 30, Institut für Statik und Stahlbau, TH Darmstadt

Führing, H., and T. Seeger (1979). Fracture Mechanics, ASTM STP 486, 144-167

Führing, H. (1980). Proceedings 2nd Conf. on Numerical Methods in Fracture Mechanics, Swansea, 645-658

Seeger, T. (1973). A contribution to the analysis of static and cyclic loaded crack sheets applying the Dugdale-Barenblatt model (in german). Report 21, Inst. für Statik u. Stahlbau, TH Darmstadt

Sippel, K. O., and D. Weisgerber (1975). Proceedings 8th ICAF Symposium, Lausanne, 7.1/1-55

Wheeler, O. E. (1972). Trans. ASME, J. Basic Eng., 181-186

Willenborg, J., R. M. Engle, and H. A. Wood (1971). A crack growth retardation model using an effective stress concept. TM71-1FBR, US-AFB, Ohio